

# Manipulations of the B-Side Charge-Separated States' Energetics in the *Rhodobacter sphaeroides* Reaction Center

Evaldas Katilius,\* Jennie L. Babendure, Zivile Katiliene, Su Lin, Aileen K. W. Taguchi, and Neal W. Woodbury

Department of Chemistry and Biochemistry and the Center for the Study of Early Events in Photosynthesis, Arizona State University, Tempe, Arizona 85287-1604

Received: April 15, 2003; In Final Form: August 25, 2003

The mutation HL(M182) in the *Rb. sphaeroides* reaction center (RC) results in the replacement of the monomer bacteriochlorophyll on the inactive side (B side) of the reaction center with a bacteriopheophytin ( $\phi_B$ ). In  $\phi_B$  containing reaction centers, excitation of the initial electron donor, the special pair P, results in about 35% electron transfer along the normally inactive B side. However, the electron is transferred only to the exchanged cofactor  $\phi_B$ . Several additional mutations in close proximity to bacteriopheophytins  $\phi_B$  or  $H_B$  have been created with the goal of altering the energetics of charge-separated states  $P^+\phi_B^-$  and  $P^+H_B^-$ . Aspartic acid residues were introduced to replace methionine L174 or valine M175 in the vicinity of the  $\phi_B$  cofactor in order to raise the free energy of state  $P^+\phi_B^-$ . Threonine M133 was mutated to the aspartic acid to add a hydrogen bond to the  $H_B$  cofactor and lower the free energy of state  $P^+H_B^-$ . The mutations in the environment surrounding the  $\phi_B$  pigment resulted in a decrease in the quantum yield of  $P^+\phi_B^-$  as well as a decrease in the recombination lifetime of this state. The mutation of valine M175 to aspartic acid showed the largest effect. The yield of state  $P^+\phi_B^-$  decreased to about 25% and its recombination lifetime shortened from 200 to 125 ps. This additional mutation also resulted in the loss of the carotenoid molecule from the reaction centers. None of the three additional mutations altered the free energies sufficiently to result in observable electron transfer to  $H_B$ . However, these measurements have allowed a more accurate assignment of the B-side charge-separated states' energetics than was previously possible.

## Introduction

The bacterial photosynthetic reaction center (RC) is a pigment protein complex that converts light energy into transmembrane charge separation.<sup>1–3</sup> The reaction center from *Rhodobacter (Rb.) sphaeroides* consists of three protein subunits L, M and H, which bind 10 cofactors: 4 bacteriochlorophylls (BChls), 2 bacteriopheophytins (BPheos), 2 quinone molecules, a carotenoid molecule, and a nonheme iron. BChl, BPheo, and quinone cofactors are arranged in two nearly symmetric branches, constituting two potential pathways for photosynthetic electron transfer (usually labeled A and B, see Figure 1). The two pathways both start with P (a pair of bacteriochlorophylls), followed by a monomer bacteriochlorophyll (either  $B_A$  or  $B_B$ ), a bacteriopheophytin (either  $H_A$  or  $H_B$ ), and then a ubiquinone (either  $Q_A$  or  $Q_B$ ). However, upon excitation of P in wild type (WT) RCs, the initial electron transfer occurs almost exclusively along the cofactors on the A side.<sup>4,5</sup> Most estimates reported in the literature for the electron-transfer ratio along the A side versus the B side in wild-type reaction centers are in the range of 30:1 to 200:1 favoring the A side.<sup>4,6–8</sup> Apparently, an electron is transferred from  $P^*$  to  $B_A$  in about 3 ps and then to  $H_A$  in less than a picosecond at room temperature.<sup>9,10</sup> Subsequently, the electron is transferred to the primary quinone acceptor,  $Q_A$ , in about 200 ps and then to the secondary quinone acceptor,  $Q_B$ , in about 200  $\mu$ s. The quantum yield of this process is near unity.<sup>11</sup>

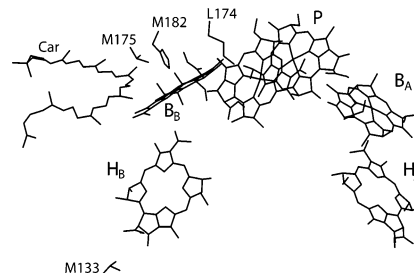


**Figure 1.** Structure of the mutated amino acid side chains and reaction center cofactors. For clarity, phytyl chains of the bacteriochlorophylls and bacteriopheophytins are removed.

One of the early studies of the electron-transfer directionality in bacterial reaction centers investigated the role of the hydrogen bond between the protein and the  $H_A$  cofactor. According to the crystal structure, glutamate L104 is within hydrogen bonding distance of the ring E keto group of the  $H_A$  molecule, whereas in the symmetry-related position, M133, next to the  $H_B$  molecule there is either a threonine (in *Rb. sphaeroides*) or a valine (in *Rb. capsulatus* and *Blastochloris (Bl.) viridis*), both of which are unable to form a hydrogen bond to  $H_B$ .<sup>12</sup> The presence of the hydrogen bond to  $H_A$  was confirmed by site-directed mutagenesis studies that showed that the hydrogen bond is responsible for the red shift of the  $Q_X$  absorbance band of  $H_A$  compared to that of  $H_B$ .<sup>13,14</sup> In addition to modifying the absorption properties of  $H_A$ , the hydrogen bond to  $H_A$  is also thought to stabilize the A-side charge-separated state  $P^+H_A^-$ . So far, there has been no experimental estimation of how much

\* Corresponding author. E-mail: Evaldas@asu.edu. Fax: (480) 965-2747.

stabilization of the charge-separated state is provided by the formation of this hydrogen bond. The results of theoretical calculations imply that the energy of state  $P^+H_A^-$  would increase by 50–60 meV if the hydrogen bond between the protein and the  $H_A$  molecule is removed.<sup>7,15</sup> One would expect that a similar stabilizing effect should be achieved by introducing a hydrogen bond to the  $H_B$  cofactor.

B-side electron-transfer kinetics were first resolved in mutants that had the primary electron acceptor  $H_A$  replaced with bacteriochlorophyll, making it possible to detect small spectral changes in the  $Q_X$  transition region of  $H_B$  (around 530 nm).<sup>16</sup> In addition to this mutation, the mutation of glycine to aspartic acid at M203 was created to modify the environment of  $B_A$  in such a way that electron transfer along the A side was greatly slowed. (Because of the difference in the subunit lengths in different strains of photosynthetic bacteria, the position of the same glycine residue is M201 in *Rb. capsulatus*; however, we will use the numbering for the *Rb. sphaeroides* strain to avoid confusion.) This facilitates the detection of B-side electron transfer, which competes with electron transfer along the A side. In such a double mutant of the *Rb. capsulatus* RC, B-side charge separation resulting in the state  $P^+H_B^-$  with a quantum yield of about 15% was observed.<sup>16</sup> B-side electron transfer was also investigated in a triple mutant, which in addition to the mutations described above also contained the mutation of valine M131 to aspartic acid.<sup>17</sup> This mutation has been shown to add a hydrogen bond to the  $H_B$  cofactor. As a result, the absorption spectra of the  $H_B$  molecule and  $H_B$  anion were red-shifted, becoming similar to the spectrum of  $H_A$ . However, the yield of state  $P^+H_B^-$  in this triple mutant did not change when compared to the yield in the double mutant, implying that the limiting factor for the B-side electron transfer was the energetics of state  $P^+B_B^-$ . This conclusion is supported by studies of other RC mutations, which stabilize the initial B-side charge-separated state, and as a consequence up to 35% yield of charge separation along the B side has been achieved.<sup>17–28</sup> All of these results show that it is possible to alter the energetics of the A- or B-side charge-separated states by mutating the protein residues surrounding the cofactors and in doing so to influence the electron-transfer pathway in the reaction center.

Previously, results were presented for HL(M182) mutant RCs in which  $B_B$  has been replaced with a BPheo (called  $\phi_B$ ). In this mutant, 35% B-side electron-transfer yield at room temperature was observed.<sup>22</sup> However, electron transfer proceeded only from  $P^*$  to  $P^+\phi_B^-$  and did not continue on to  $P^+H_B^-$ . Subsequent analysis showed that in this mutant the free energy of state  $P^+\phi_B^-$  was significantly below that of both  $P^*$  and  $P^+H_B^-$ , making further electron transfer from  $\phi_B$  to  $H_B$  improbable.<sup>23</sup> On the basis of these previous results, several secondary mutations in addition to the HL(M182) mutation have been introduced in order to alter the energies of the B-side charge-separated states and to explore the energetic dependence of the B-side electron-transfer reactions. Methionine at position L174, which was the symmetry-related residue to glycine M203<sup>12</sup> and thus close to  $B_B$  (or  $\phi_B$ ), was changed to aspartic acid (mutation MD(L174)), and valine at position M175, which was also in close proximity to  $B_B$  (or  $\phi_B$ ), was changed to aspartic acid (mutation VD(M175)) to investigate the effects of increasing the free energy of state  $P^+\phi_B^-$ . Also, a threonine M133-to-aspartate mutation (mutation TD(M133)) was introduced to create a hydrogen bond to the  $H_B$  cofactor (Figure 1). In principle, this should lower the energy of the state  $P^+H_B^-$  relative to that of the state  $P^+\phi_B^-$ . The properties of these three

double mutants and the implications for the energetics of the B-side charge-separated states will be discussed.

## Materials and Methods

All mutations were created using a QuikChange mutagenesis kit (Stratagene). In the case of the M subunit mutants, the mutagenesis reactions were performed on the plasmid pUCHBH7M182HL, which consisted of the plasmid pUC19 with the *HindIII*-*Bam*HI fragment of the M protein subunit gene containing the HL(M182) mutation.<sup>22,23</sup> Also, at the end of the M subunit gene, a His-tag sequence has been added (repeat of seven CAC codons encoding seven His amino acids).<sup>23,29</sup> In the case of the L subunit mutations, the mutagenesis reactions were performed on plasmid pUCAH, which was made up of pUC19 with the *Asp*718I-*HindIII* fragment of the L subunit gene.<sup>30</sup> The mutagenesis reactions were performed according to the kit manual, and the mutations were verified by DNA sequencing of the whole fragment of the L or M subunit genes. Then the fragments of the genes were subcloned into the plasmid pRKSch.<sup>30</sup> In case of the L subunit mutation, the fragment containing the MD(L174) mutation was subcloned into the pRKSchM182HL plasmid, which contained the HL(M182) mutation. Those plasmids were then transferred by conjugation into the *Rb. sphaeroides* *pufLM* deletion strain  $\Delta$ LM1.1, which lacked the reaction center gene.<sup>30</sup> Cells were grown and reaction centers were isolated according to previously described procedures.<sup>23</sup> The sample preparation for transient absorbance measurements as well as the experimental setup have also been described in previous publications.<sup>22,23</sup>

## Results

**Pigment Ratio Analysis.** The bacteriochlorophyll-to-bacteriopheophytin ratio was analyzed in all double mutants to make sure that the introduced mutations did not alter the pigment ratio compared to the HL(M182) mutation alone. In all of the double mutants, the ratio of the BChl to BPheo pigments was  $1.1 \pm 0.1$ , which was essentially the same as in the HL(M182) mutant RCs. In addition, in the VD(M175) + HL(M182) mutant, an apparent loss of the carotenoid from the reaction centers was detected in the pigment extractions as the disappearance of the characteristic carotenoid absorbance bands in the 500-nm region.

**Room-Temperature Absorption Spectra.** The absorption spectra of double-mutant RCs MD(L174) + HL(M182), VD(M175) + HL(M182), and TD(M133) + HL(M182) as well as that of the HL(M182) mutant RC at room temperature are shown in Figure 2. As previously described,<sup>22</sup> the replacement of  $B_B$  with  $\phi_B$  caused the spectral features usually associated with the  $B_B$  molecule to disappear and new spectral features associated with the exchanged bacteriopheophytin molecule to appear. In particular, the low-energy side of the B band around 807 nm disappeared while at the same time a new band associated with  $\phi_B$  appeared at around 785 nm. The change of BChl to BPheo was also clearly defined in the  $Q_X$  spectral region, where the absorption intensity of the BChl band at 600 nm decreased and the intensity of the BPheo band around 540 nm increased.<sup>22</sup>

Each of the secondary mutations introduces additional changes into the HL(M182) absorption spectrum. Perhaps the least-visible effect is caused by mutation TD(M133), which is designed to add a hydrogen bond to the  $H_B$  molecule. As a result of that mutation, the spectrum of the  $H_B$  cofactor red-shifts by 4–5 nm (Figure 2), which is well resolvable in the BPheo  $Q_X$  band at low temperatures (see below).

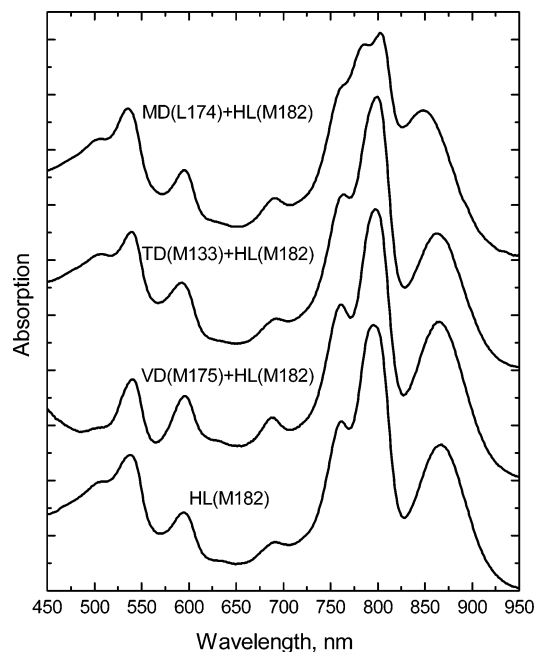


**Figure 2.** Absorption spectra of MD(L174) + HL(M182), TD(M133) + HL(M182), VD(M175) + HL(M182), and HL(M182) mutant RCs at room temperature.

The absorption spectrum of the VD(M175) + HL(M182) mutant in the BChl and BPheo regions is quite similar to the spectrum of the HL(M182) mutant, although a small narrowing and slight increase in the intensity of the band at around 797 nm can be resolved, indicating a red shift of the  $\phi_B$   $Q_Y$  band. The spectrum of this mutant also shows that the carotenoid absorption band is largely missing, suggesting that a large fraction of the carotenoid normally present in the RC is absent. The loss of carotenoid can be explained by the fact that valine M175 is one of the residues that make up the carotenoid binding site. Apparently, the mutation of valine to aspartate results in steric hindrance or alters the hydrophobic properties of the carotenoid binding site. The absorption spectrum of the VD(M175) + HL(M182) mutant is similar to that of mutation GL(M71), which has also been shown to remove the carotenoid from its binding site.<sup>31</sup>

The most pronounced change in the room-temperature absorption spectrum, compared to that of HL(M182) alone, is caused by the addition of mutation MD(L174). In this double mutant, the spectrum of the  $\phi_B$  molecule is clearly separated from the  $B_A$  absorption band, resulting in two peaks at 803 and 786 nm. In addition to that, the spectrum of the special pair is also affected; the peak of the P absorbance band is shifted from 865 nm to about 847 nm. In contrast, the  $Q_X$  region remains practically unchanged compared to that of the HL(M182) mutant. Similar blue shifts of the  $B_B$  and P ground-state absorption bands have also been observed in the spectrum of ID(L177) mutant RCs. This mutation placed an aspartic acid residue in the vicinity of the  $B_B$  and P cofactors.<sup>32</sup>

**Absorption Spectra at 77 K.** To better resolve the band shifts associated with the secondary mutations, absorption spectra of the double mutants were also measured at 77 K. Low-temperature absorption spectra are shown in Figure 3. As already mentioned above, mutation TD(M133) altered only the properties of the  $H_B$   $Q_X$  absorption band. At 77 K, the  $Q_X$  absorption band of  $H_B$  is red-shifted by about 4–5 nm; it becomes a shoulder on the  $H_A$  absorbance band at 545 nm. The red shift of the  $H_B$  transitions observed in the spectrum of the TD(M133) + HL(M182) mutant (Figures 2 and 3) is consistent with

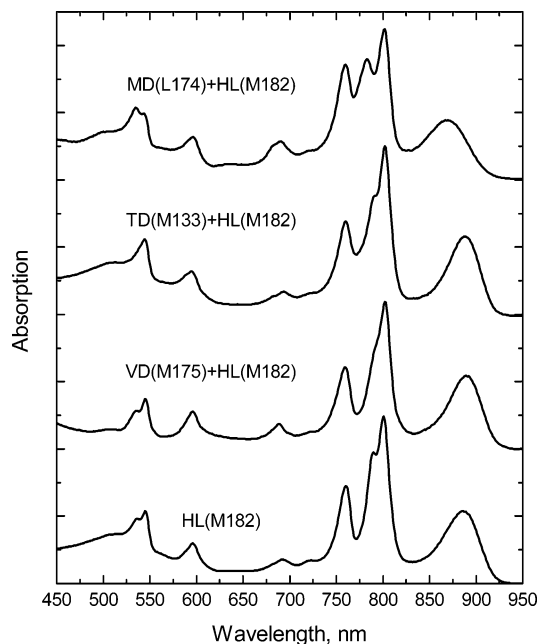


**Figure 3.** Absorption spectra of MD(L174) + HL(M182), TD(M133) + HL(M182), VD(M175) + HL(M182), and HL(M182) mutant RCs at 77 K.

previous results for the mutation TD(M133) alone in *Rb. sphaeroides*.<sup>33</sup> An analogous mutation, VD(M133), has also been created in *Rb. capsulatus* RC,<sup>17</sup> but the addition of the hydrogen bond to  $H_B$  in this species does not induce an observable shift of the  $H_B$  ground-state absorption band. However, a red shift in the VD(M133) *Rb. capsulatus* mutant is observed in the bleaching of the  $H_B$   $Q_X$  band as well as in the  $H_B$  anion band in transient absorption spectra.<sup>17</sup>

From the low-temperature absorption spectrum, it is apparent that the addition of mutation VD(M175) to HL(M182) slightly alters the spectral properties of the  $\phi_B$  molecule. Mutation VD(M175) causes about a 5-nm red shift of the  $Q_Y$  absorption band of  $\phi_B$ ; however, there is no significant effect in the  $Q_X$  transition region around 540 nm. The low-temperature spectrum of the MD(L174) + HL(M182) mutant RCs is also shown in Figure 3 and demonstrates that the blue shifts of the  $\phi_B$  and P absorption bands described above become more pronounced at low temperature. At 77 K, the P band is blue-shifted by about 20 nm compared to the position of the P band in HL(M182) mutant RCs. The absorption of the  $\phi_B$  molecule is also blue-shifted in this mutant such that its  $Q_Y$  band is positioned near 782 nm instead of 790 nm as in the HL(M182)-only mutant RCs. A similar shift is observed in the  $Q_X$  band of  $\phi_B$  in the MD(L174) + HL(M182) mutant RCs as well. As a result, it overlaps the absorption band of the  $H_B$  molecule at 535 nm (Figure 3).

**Photochemical Properties of Double Mutants.** Transient absorption measurements were performed on all double mutants to investigate the changes in the primary photochemistry of the RCs. As previously reported for HL(M182) mutant RCs, two different charge-separated states,  $P^+\phi_B^-$  and  $P^+H_A^-$ , are formed upon direct excitation of P. The altered properties of the HL(M182) mutant RCs are reflected in the  $P^*$  stimulated emission decay, which in the mutant is about 20% faster than in WT RCs:  $2.6 \pm 0.1$  and  $3.1 \pm 0.2$  ps for HL(M182) and WT RCs, respectively.<sup>22</sup> The results of the  $P^*$  stimulated emission decays for all double mutants are presented in Table 1. The decay kinetics of  $P^*$  in the TD(M133) + HL(M182) mutant RCs are essentially the same as in HL(M182) alone.



**TABLE 1: Properties of Mutant RCs**

sample	$\tau_{P^*}$ , ps	lifetime of $P^+\phi_B^-$ decay, ps	yield of $P^+\phi_B^-$ , %
MD(L174) + HL(M182)	$3.0 \pm 0.1$	$170 \pm 5$	$28 \pm 4$
TD(M133) + HL(M182)	$2.7 \pm 0.1$	$190 \pm 10$	$33 \pm 3$
VD(M175) + HL(M182)	$3.2 \pm 0.1$	$125 \pm 3$	$25 \pm 2$
HL(M182)	$2.6 \pm 0.1$	$200 \pm 20$	$35 \pm 5$
WT	$3.1 \pm 0.2$		

This is expected because the additional mutation is close to  $H_B$ ; therefore, it should not significantly alter the properties of P or  $\phi_B$ . In the case of the mutant MD(L174) + HL(M182), the  $P^*$  decay is slightly longer than that for HL(M182) alone. The lifetime of  $P^*$  decay in the VD(M175) + HL(M182) mutant is the same as the decay time found in WT RCs. Possible reasons for the observed increase in the  $P^*$  lifetime in these mutants will be discussed below.

As mentioned above, in the HL(M182) mutant, B-side electron transfer occurs only as far as state  $P^+\phi_B^-$ . The yield of that state at room temperature is about 35%, and the remaining 65% of the electron transfer forms state  $P^+H_A^-$ . The decay time constants for the two states are quite different:  $P^+\phi_B^-$  decays with a 200-ps lifetime, but  $P^+H_A^-$  decays on the 10-ns time scale.<sup>22</sup> Thus, the relative yield of the electron transfer on the B side versus that on the A side in this mutant can be determined by comparing the intensity of the P-band bleaching in the nanosecond decay-associated spectrum (A side) with the P-band bleaching in the 200-ps decay-associated spectrum (B side). The same analysis was performed in all of the double mutants. The lifetimes and the yields of state  $P^+\phi_B^-$  in all mutants are summarized in Table 1. As one can see, in the case of the TD(M133) + HL(M182) mutant, both the lifetime and the yield of state  $P^+\phi_B^-$  are essentially the same as in the HL(M182) mutant. There is also no indication of further electron transfer to  $H_B^-$ ; no long-lived  $H_B$  band bleaching at 530 nm or  $H_B$  anion absorption band near 630 nm is observed in the transient spectra at long times (data not shown). Thus, we can conclude that the addition of the TD(M133) mutation did not lower the energy of state  $P^+H_B^-$  enough relative to the free energy of state  $P^+\phi_B^-$  to observe additional electron transfer from  $\phi_B$  to  $H_B$ .

In the other two mutants, which have mutations near the  $\phi_B$  pigment, more significant changes are observed in both the lifetime and yield of charge-separated state  $P^+\phi_B^-$ . In the case of the mutant MD(L174) + HL(M182), the yield and the lifetime of this state decrease slightly compared to those of the HL(M182) mutant. The yield in this mutant decreases to about 28%, and the lifetime for the  $P^+\phi_B^-$  decay shortens to about 170 ps (Table 1 and Figure 4a). It should be noted that the decay-associated spectrum corresponding to the decay of the  $P^+\phi_B^-$  state in the MD(L174) + HL(M182) mutant reaction centers shows a blue shift of the  $\phi_B$  bleaching compared to the spectrum of the HL(M182) reaction centers. The shifted position of the bleaching at 780 nm in this mutant correlates to the position of the  $\phi_B$  absorption band observed in the 77 K ground-state spectrum (Figure 3).

Larger changes are observed in the mutant VD(M175) + HL(M182). In this mutant, the yield of state  $P^+\phi_B^-$  decreases to about 25%, and its decay lifetime decreases to about 125 ps (Figure 4b). It is interesting that the decay-associated spectrum of the 125-ps component shows the bleaching of a band around 795 nm instead of 787 nm as observed in the HL(M182) mutant. The spectral shift of the  $\phi_B$  bleaching is again correlated to the observed shift of the  $\phi_B$  ground-state absorption band in the 77 K spectrum (Figure 3). In the ground-state absorption spectrum

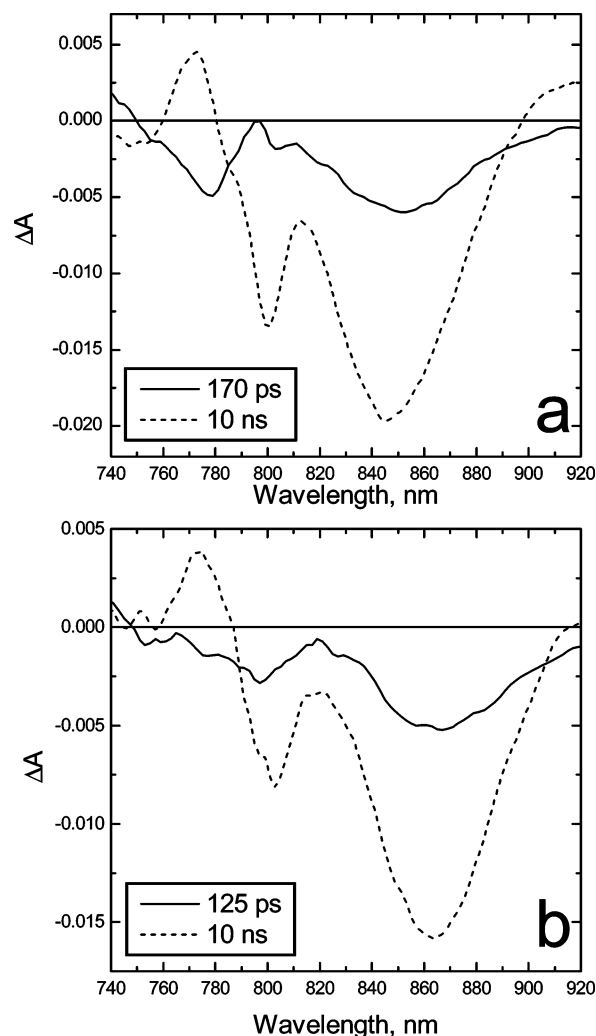


**Figure 4.** Decay-associated spectra corresponding to states  $P^+\phi_B^-$  and  $P^+H_A^-$  in the MD(L174) + HL(M182) and VD(M175) + HL(M182) mutant RCs at room temperature. (a) Decay-associated spectra of MD(L174) + HL(M182) mutant RCs. The spectra were obtained from a global fit of 1-ns time scale transient absorbance data with the two exponential decays terms having lifetimes of 170 ps and 10 ns. For these measurements,  $Q_A$  was prerduced with 1 mM sodium dithionite, and the sample was excited at 850 nm. (b) Decay-associated spectra of VD(M175) + HL(M182) mutant RCs. The spectra were obtained from a global fit of 1-ns time scale transient absorbance data using two exponential decay components with lifetimes of 125 ps and 10 ns. The quinone,  $Q_A$ , was prerduced, and excitation was at 865 nm.

at room temperature, the shift is not well resolved because the  $\phi_B$  and  $B_A$  bands overlap (although some narrowing and a slight increase in the intensity of the band near 797 nm is observed, indicating the shift of the  $\phi_B$  band (Figure 2)).

It is apparent from the results described above that the placement of aspartic acid residues in the vicinity of the  $\phi_B$  molecule influences the initial B-side electron transfer as well as the recombination of the  $P^+\phi_B^-$  state. However, in none of the mutants is  $P^+H_B^-$  formation observed upon the decay of  $P^+\phi_B^-$  (i.e., no long-lived spectral features corresponding to the  $H_B$  anion are detected in the transient spectra).

## Discussion

Mutation HL(M182) has been previously shown to allow B-side electron transfer from  $P^*$  to effectively compete with normal A-side electron transfer in bacterial photosynthetic reaction centers from *Rb. sphaeroides*.<sup>22,23</sup> This is possible

because the mutation results in the replacement of the B-side monomer bacteriochlorophyll with a bacteriopheophytin, greatly stabilizing the initial charge-separated state on the B side. In fact, this initial B-side charge-separated state,  $P^+\phi_B^-$ , apparently has a lower free energy than  $P^+H_B^-$ , and thus additional electron transfer along the B-side pathway (Figure 1) does not occur. In the current work, three different mutations have been combined with the HL(M182) mutation to probe the energetics of the B-side electron-transfer process further.

**Effects of Mutations on Electron-Transfer Kinetics.** Excitation of the HL(M182) mutant RCs at room temperature gives rise to electron transfer on the B side of the reaction center, forming state  $P^+\phi_B^-$  with a yield of 35%.<sup>22</sup> The availability of the B-side electron-transfer pathway in this mutant is also reflected in the decrease of the  $P^*$  decay lifetime compared to the  $P^*$  lifetime in WT RCs. The three additional mutations introduced as part of the present work should either increase the standard free energy of state  $P^+\phi_B^-$  or decrease the free energy of  $P^+H_B^-$ , depending on the mutation. In TD(M133) + HL(M182) RCs, it was expected that a hydrogen bond would be formed between the introduced aspartic acid and  $H_B$ , stabilizing the anion of  $H_B$  just as the hydrogen bond between glutamic acid L104 and  $H_A$  is thought to stabilize the  $H_A$  anion.<sup>7,15</sup> Given that the initial charge-separation reaction on the B side does not involve  $H_B$ , one would not expect this mutation to have substantial effects on the kinetics of  $P^*$  decay, and indeed the  $P^*$  decay kinetics in the double mutant are essentially the same as in HL(M182) alone. The other two mutations (VD(M175) and MD(L174)) alter the environment of  $\phi_B$ , and the increase in the  $P^*$  decay kinetics is observed compared to the kinetics of the HL(M182) mutation alone. The introduction of a negative charge near  $\phi_B$  is expected to increase the free energy of the  $P^+\phi_B^-$  state, thus the increase in the  $P^*$  decay time and the decrease of the  $P^+\phi_B^-$  yield can be explained by a corresponding decrease in the B-side electron-transfer rate. Destabilization of state  $P^+\phi_B^-$  can also result in a greater driving force for recombination to the ground state and therefore a decrease in the lifetime of the state  $P^+\phi_B^-$  in the MD(L174) + HL(M182) and VD(M175) + HL(M182) mutant RCs.

**Effects of Mutations on the Energetics of B-Side Charge-Separated States.** Previously, it has been estimated that the standard free energy of the charge-separated state  $P^+\phi_B^-$  is about  $0.16 \pm 0.04$  eV below  $P^*$ .<sup>23</sup> Prior estimates of the standard free energy of the state  $P^+H_B^-$  have placed it between 0 and 70 meV below  $P^*$ .<sup>26</sup> Theoretical calculations based on the *Bl. viridis* crystal structure are in line with this estimate, placing the free energy of state  $P^+H_B^-$  about 100–200 meV above that of  $P^+H_A^-$ ,<sup>7,15,34</sup> which is thought to be approximately 0.15–0.25 eV below  $P^*$ .<sup>35–40</sup> Most of the energetic difference between the  $P^+H_A^-$  and  $P^+H_B^-$  states is attributed to the favorable interactions of the  $H_A$  molecule with glutamic acid L104,<sup>7,15</sup> which makes the hydrogen bond to the ring E keto group of the  $H_A$  molecule.<sup>13,41,42</sup> The replacement of threonine with aspartic acid at position M133 has previously been proposed to add a hydrogen bond to  $H_B$  in *Rb. sphaeroides* RCs.<sup>33</sup> (The introduction of the hydrogen bond by analogous mutation VD(M131) in *Rb. capsulatus* RCs has been shown by measurements of resonance Raman spectra.<sup>17</sup>) In the case of the TD(M133) mutation studied here, one might expect state  $P^+H_B^-$  to be stabilized by about 50–60 meV.<sup>7,15</sup> This may not be sufficient to decrease the free energy of  $P^+H_B^-$  to a level below  $P^+\phi_B^-$ , taking into account the free-energy estimates for the two states (Figure 5). Also, the stabilization of the  $P^+H_B^-$  state due to the addition of the hydrogen bond might not be as great

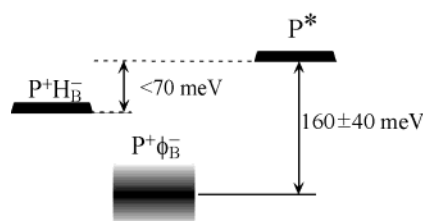


**Figure 5.** Standard free-energy diagram for the B-side charge-separated states in the HL(M182) mutant RC. The value of the free-energy gap between the  $P^*$  and  $P^+\phi_B^-$  states is as determined in ref 23. The value of the free-energy gap between  $P^*$  and  $P^+H_B^-$  is based on recently published results<sup>26</sup> and is consistent with the results from the mutant RCs in this study.

as predicted from the theoretical calculations, or the mutation might not create the hydrogen bond between the protein and  $H_B$  cofactor. (Even though the  $Q_X$  absorption band is affected by the mutation, the formation of the hydrogen bond has never been confirmed in *Rb. sphaeroides* RCs.) In any case, mutation TD(M133), which is meant to introduce the hydrogen bond to  $H_B$ , does not provide sufficient stabilization of the state  $P^+H_B^-$  to decrease its energy below the energy of the  $P^+\phi_B^-$  state.

Mutations in the proximity of the  $\phi_B$  molecule have been introduced with the intention of increasing the free energy of state  $P^+\phi_B^-$ . Previously, it has been suggested that placing an aspartic acid next to  $B_A$  (mutation GD(M203)) results in an increase in the free energy of  $P^+B_A^-$  by as much as 100–150 meV.<sup>16,43</sup> This destabilization of  $P^+B_A^-$  is reflected in the decrease in the primary electron-transfer rate both in *Rb. sphaeroides* and *Rb. capsulatus* RCs.<sup>16,21,32,43</sup> Resonance Raman results suggested that the aspartic acid at position M203 must be at least partially negatively charged, causing the energy of state  $P^+B_A^-$  to increase.<sup>44</sup> However, no experimental evaluation of the free energy of state  $P^+B_A^-$  in this mutant has been reported.

Two secondary mutations placing aspartic acids in the background of the HL(M182) mutation were created to increase the standard free energy of  $P^+\phi_B^-$ . Both mutations were expected to destabilize charge-separated state  $P^+\phi_B^-$ , possibly leading to additional electron transfer from  $P^+\phi_B^-$  to  $P^+H_B^-$ . However, electron transfer to  $H_B$  was not observed, even though the mutations apparently resulted in the destabilization of state  $P^+\phi_B^-$ , as described below.

In the VD(M175) + HL(M182) mutant, the B-side electron-transfer rate clearly decreased, resulting in a decreased yield of  $P^+\phi_B^-$  as well as an increase in the recombination rate of  $P^+\phi_B^-$ . All of these changes are consistent with the destabilization of the  $P^+\phi_B^-$  state due to the placement of a negatively charged residue close to the  $\phi_B$  molecule. As mentioned above, placing aspartic acid next to  $B_A$  was supposed to increase the free energy of state  $P^+B_A^-$  by about 100–150 meV.<sup>16,43</sup> Assuming the same magnitude effect as a result of the VD(M175) mutation, the state  $P^+\phi_B^-$  then would be nearly isoenergetic with  $P^+H_B^-$  or even  $P^*$  (Figure 5). However, no evidence for  $H_B$  anion formation in this double mutant is detected, suggesting that the free energy of  $P^+H_B^-$  is still unfavorable relative to the free energy of  $P^+\phi_B^-$ . Considering the estimated free energy of  $P^+\phi_B^-$  in the HL(M182)-only mutant (about  $0.16 \pm 0.04$  eV below  $P^*$ ), a destabilization of  $P^+\phi_B^-$  by 100 meV due to the introduction of a negatively charged residue near  $\phi_B$  could still leave a significant energetic barrier for additional B-side electron transfer to  $H_B$  if either  $P^+\phi_B^-$  was close to 0.2 eV below  $P^*$  or if  $P^+H_B^-$  was nearly isoenergetic with  $P^*$ . Another possibility is that the introduced aspartic acid does not generate as large of an effect on the energetics of the B-side charge-separated

states as previously suggested for the A-side mutations in *Rb. capsulatus* RCs.<sup>16,43</sup>

The same reasoning could be applied to the MD(L174) + HL(M182) mutant. In this mutant, there is also a slight decrease in the  $P^+\phi_B^-$  yield as well as an increase in the recombination rate. Mutation MD(L174) produces effects similar to those of the mutation GD(M203); however, its absolute effect on the energetics of the state  $P^+\phi_B^-$  is likely smaller than that estimated for  $P^+B_A^-$  in the previously studied mutants of *Rb. capsulatus*.<sup>16,43</sup> Of course, one cannot exclude the possibility that the mutations studied here decrease the electronic coupling between the  $\phi_B$  and  $H_B$  pigments, making the electron transfer between the two cofactors improbable, though in other characterized mutations that affect B-side transfer the energetics appeared to play the dominant role.<sup>16,17,20,23,26</sup>

The results of the double mutants studied in this work confirm previous estimates for the energetics of the B-side charge-separated states in the *Rb. sphaeroides* reaction center. However, none of the mutations used here resulted in a large enough change in the relative free energies of the B-side charge-separated states to allow electron transfer from  $\phi_B$  to  $H_B$ . One might think that generating a triple mutant consisting of HL(M182), TD(M133), and VD(M175) would result in a favorable free-energy change between  $P^+\phi_B^-$  and  $P^+H_B^-$ . This triple mutant, TD(M133) + VD(M175) + HL(M182), was created to test this hypothesis, but the resulting RCs were apparently not stable; the mutated bacteria were unable to grow photosynthetically, and no intact RCs could be isolated.

**Acknowledgment.** This research was supported by NSF grant MCB0131766. The transient spectrometer that was used was funded by NSF grant BIR9512970. This is publication no. 572 from the Center for the Study of Early Events in Photosynthesis.

## References and Notes

- Hoff, A. J.; Deisenhofer, J. *Phys. Rep.* **1997**, 287, 1.
- Parson, W. W. Photosynthetic Bacterial Reaction Centres. In *Protein Electron Transfer*; Bendall, S. D., Ed.; BIOS Scientific Publishers: Oxford, U.K., 1996; p 125.
- Woodbury, N. W.; Allen, J. P. The Pathway, Kinetics and Thermodynamics of Electron Transfer in Wild Type and Mutant Reaction Centers of Purple Nonsulfur Bacteria. In *Anoxygenic Photosynthetic Bacteria*; Blankenship, R. E., Madigan, M. T., Bauer, C. E., Eds.; Kluwer Academic Publishers: Dordrecht, The Netherlands, 1995; Vol. 2, p 527.
- Kirmaier, C.; Holten, D.; Parson, W. W. *Biochim. Biophys. Acta* **1985**, 810, 49.
- Kirmaier, C.; Holten, D.; Parson, W. W. *Biochim. Biophys. Acta* **1985**, 810, 33.
- Kellogg, E. C.; Kolaczowski, S.; Wasielewski, M. R.; Tiede, D. M. *Photosynth. Res.* **1989**, 22, 47.
- Michel-Beyerle, M. E.; Plato, M.; Deisenhofer, J.; Michel, H.; Bixon, M.; Jortner, J. *Biochim. Biophys. Acta* **1988**, 932, 52.
- Tiede, D. M.; Kellogg, E.; Breton, J. *Biochim. Biophys. Acta* **1987**, 892, 294.
- Holzappel, W.; Finkle, U.; Kaiser, W.; Oesterhelt, D.; Scheer, H.; Stolz, H. U.; Zinth, W. *Chem. Phys. Lett.* **1989**, 160, 1.
- Sporlein, S.; Zinth, W.; Meyer, M.; Scheer, H.; Wachtveitl, J. *Chem. Phys. Lett.* **2000**, 322, 454.
- Wraight, C. A.; Clayton, R. K. *Biochim. Biophys. Acta* **1973**, 333, 246.
- Komiya, H.; Yeates, T. O.; Rees, D. C.; Allen, J. P.; Feher, G. *Proc. Natl. Acad. Sci. U.S.A.* **1988**, 85, 9012.
- Bylina, E. J.; Kirmaier, C.; McDowell, L.; Holten, D.; Youvan, D. C. *Nature* **1988**, 336, 182.
- Coleman, W. J.; Youvan, D. C. *Annu. Rev. Biophys. Biophys. Chem.* **1990**, 19, 333.
- Parson, W. W.; Chu, Z.-T.; Warshel, A. *Biochim. Biophys. Acta* **1990**, 1017, 251.
- Heller, B. A.; Holten, D.; Kirmaier, C. *Science* **1995**, 269, 940.
- Kirmaier, C.; Cua, A.; He, C.; Holten, D.; Bocian, D. F. *J. Phys. Chem. B* **2002**, 106, 495.
- Kirmaier, C.; Weems, D.; Holten, D. *Biochemistry* **1999**, 38, 11516.
- Roberts, J. A.; Holten, D.; Kirmaier, C. *J. Phys. Chem. B* **2001**, 105, 5575.
- Kirmaier, C.; He, C.; Holten, D. *Biochemistry* **2001**, 40, 12132.
- Kirmaier, C.; Laible, P. D.; Czarnecki, K.; Hata, A. N.; Hanson, D. K.; Bocian, D. F.; Holten, D. *J. Phys. Chem. B* **2002**, 106, 1799.
- Katilius, E.; Turanchik, T.; Lin, S.; Taguchi, A. K. W.; Woodbury, N. W. *J. Phys. Chem. B* **1999**, 103, 7386.
- Katilius, E.; Katiliene, Z.; Lin, S.; Taguchi, A. K. W.; Woodbury, N. W. *J. Phys. Chem. B* **2002**, 106, 1471.
- de Boer, A. L.; Neerken, S.; de Wijn, R.; Permentier, H. P.; Gast, P.; Vijgenboom, E.; Hoff, A. J. *Biochemistry* **2002**, 41, 3081.
- de Boer, A. L.; Neerken, S.; de Wijn, R.; Permentier, H. P.; Gast, P.; Vijgenboom, E.; Hoff, A. J. *Photosynth. Res.* **2002**, 71, 221.
- Katilius, E.; Katiliene, Z.; Lin, S.; Taguchi, A. K. W.; Woodbury, N. W. *J. Phys. Chem. B* **2002**, 106, 12344.
- Kirmaier, C.; Laible, P. D.; Hanson, D. K.; Holten, D. *Biochemistry* **2003**, 42, 2016.
- Laible, P. D.; Kirmaier, C.; Udawatte, C. S. M.; Hofman, S. J.; Holten, D.; Hanson, D. K. *Biochemistry* **2003**, 42, 1718.
- Goldsmith, J. O.; Boxer, S. G. *Biochim. Biophys. Acta* **1996**, 1276, 171.
- Lin, X.; Williams, J. C.; Allen, J. P.; Mathis, P. *Biochemistry* **1994**, 33, 13517.
- Ridge, J. P.; van Brederode, M. E.; Goodwin, M. G.; van Grondelle, R.; Jones, M. R. *Photosynth. Res.* **1999**, 59, 9.
- Williams, J. C.; Alden, R. G.; Murchison, H. A.; Peloquin, J. M.; Woodbury, N. W.; Allen, J. P. *Biochemistry* **1992**, 31, 11029.
- Muh, F.; Williams, J. C.; Allen, J. P.; Lubitz, W. *Biochemistry* **1998**, 37, 13066.
- Gunner, M. R.; Nicholls, A.; Honig, B. *J. Phys. Chem.* **1996**, 100, 4277.
- Ogrodnik, A.; Keupp, W.; Volk, M.; Aumeier, G.; Michel-Beyerle, M. E. *J. Phys. Chem.* **1994**, 98, 3432.
- Ogrodnik, A.; Volk, M.; Letterer, R.; Feick, R.; Michel-Beyerle, M. E. *Biochim. Biophys. Acta* **1988**, 936, 361.
- Ogrodnik, A.; Hartwich, G.; Lossau, H.; Michel-Beyerle, M. E. *Chem. Phys.* **1999**, 244, 461.
- Peloquin, J. M.; Williams, J. C.; Lin, X.; Alden, R. G.; Murchison, H. A.; Taguchi, A. K. W.; Allen, J. P.; Woodbury, N. W. *Biochemistry* **1994**, 33, 8089.
- Schenck, C. C.; Blankenship, R. E.; Parson, W. W. *Biochim. Biophys. Acta* **1982**, 680, 44.
- Woodbury, N. W. T.; Parson, W. W. *Biochim. Biophys. Acta* **1984**, 767, 345.
- Ermiler, U.; Fritzsche, G.; Buchanan, S. K.; Michel, H. *Structure* **1994**, 2, 925.
- Allen, J. P.; Feher, G.; Yeates, T. O.; Komiya, H.; Rees, D. C. *Proc. Natl. Acad. Sci. U.S.A.* **1988**, 85, 8487.
- Heller, B. A.; Holten, D.; Kirmaier, C. *Biochemistry* **1996**, 35, 15418.
- Czarnecki, K.; Kirmaier, C.; Holten, D.; Bocian, D. F. *J. Phys. Chem. A* **1999**, 103, 2235.